

# Manual Design and Evaluation of Butterworth and Chebyshev-I Digital IIR Filters with Application to ECG Denoising

Ariasu Florian-Andrei

*Facultatea de Automatica si Calculatoare*

*Universitatea Nationala de Stiinta si Tehnologie Politehnica Bucuresti*

Bucuresti, Romania

ariasu.florian@yahoo.com

**Abstract**—This work presents a manual design procedure for low-pass Butterworth and Chebyshev-I digital IIR filters, starting from amplitude and frequency specifications and following the classical analog-prototype to bilinear-transform workflow. The resulting filters are implemented in Python and validated in two stages: (i) on a synthetic test signal composed of a low-frequency sinusoid, high-frequency interference and white noise, and (ii) on a real ECG recording from the MIT-BIH arrhythmia database. Magnitude, phase and pole-zero plots are analyzed together with a selectivity metric and region of convergence (ROC), and time/frequency-domain results are used to compare the denoising performance of the two filters.

**Index Terms**—digital filters, IIR, Butterworth, Chebyshev, bilinear transform, ECG denoising

## I. INTRODUCTION

Digital filters are fundamental tools for separating useful components from interference and noise in discrete-time signals. Low-pass infinite impulse response (IIR) filters are particularly attractive when a steep transition band is needed with a relatively low filter order. Butterworth and Chebyshev-I prototypes are two classical choices with complementary properties: Butterworth provides a maximally flat passband, while Chebyshev-I achieves higher selectivity at the cost of passband ripple [1].

This paper documents the complete workflow of manually designing, implementing and evaluating Butterworth and Chebyshev-I low-pass IIR filters in Python. The design follows the standard sequence: specification of passband and stopband constraints, derivation of analog prototypes in the  $s$ -plane, mapping to the  $z$ -plane by bilinear transform, then application to synthetic and real signals.

## II. FILTER DESIGN METHODOLOGY

### A. Amplitude and Frequency Specifications

Each low-pass filter is specified by:

- passband ripple  $\delta_p$  and the corresponding  $R_p = 20 \log_{10}(\delta_p)$  [dB];
- minimum stopband attenuation  $\delta_s$  and  $R_s = 20 \log_{10}(\delta_s)$  [dB];
- passband edge frequency  $f_p$  and stopband edge frequency  $f_s$ ;

- sampling frequency  $F_s$  and Nyquist frequency  $F_N = F_s/2$ .

For the synthetic test case, the parameters are  $\delta_p = 0.5$ ,  $\delta_s = 34$ ,  $f_p = 10$  kHz,  $f_s = 14$  kHz and  $F_s = 50$  kHz.

### B. Manual Analog Butterworth Design

The function `butter_manual` implements the manual Butterworth design. From the amplitude specifications, it computes

$$R_p = 20 \log_{10}(\delta_p), \quad R_s = 20 \log_{10}(\delta_s),$$

then the analog passband and stopband pulsations

$$\omega_p = 2\pi f_p, \quad \omega_s = 2\pi f_s.$$

The minimum filter order  $N$  is obtained from the classical Butterworth relation

$$N = \left\lceil \frac{\log_{10} \left( \frac{10^{R_s/10} - 1}{10^{R_p/10} - 1} \right)}{\log_{10}(\omega_s/\omega_p)} \right\rceil.$$

Normalized Butterworth poles lie on a circle of radius 1 in the left half of the  $s$ -plane. The code generates all  $N$  roots, keeps only the poles with negative real part and then scales them to the prewarped cutoff  $\tilde{\omega}_p$ .

### C. Manual Analog Chebyshev-I Design

The function `cheby1_manual` follows the standard Chebyshev-I prototype design. From  $R_p$ , it computes

$$\varepsilon = \sqrt{10^{R_p/10} - 1},$$

and derives the order

$$N = \left\lceil \frac{\operatorname{arccosh} \left( \sqrt{\frac{10^{R_s/10} - 1}{10^{R_p/10} - 1}} \right)}{\operatorname{arccosh}(\omega_s/\omega_p)} \right\rceil.$$

The Chebyshev-I poles are distributed on an ellipse in the left half-plane. With

$$\alpha = \frac{1}{N} \operatorname{arcsinh} \left( \frac{1}{\varepsilon} \right),$$

each pole is obtained as

$$\begin{aligned}\sigma_k &= -\sinh(\alpha) \sin \theta_k, & \omega_k &= \cosh(\alpha) \cos \theta_k, \\ p_k &= \tilde{\omega}_p (\sigma_k + j\omega_k),\end{aligned}$$

again keeping only poles with negative real part.

#### D. Bilinear Transform and Digital Realization

Both analog prototypes are converted to digital filters by the bilinear transform. Frequency prewarping is applied as

$$\tilde{\omega}_p = \frac{2}{T} \tan\left(\frac{\Omega_p}{2}\right), \quad T = \frac{1}{F_s}, \quad \Omega_p = 2\pi \frac{f_p}{F_s}.$$

The mapping  $s = \frac{2(1-z^{-1})}{T(1+z^{-1})}$  preserves stability and maps the analog frequency axis to the unit circle. In Python, the mapping from analog zeros, poles and gain to digital form is performed with `bilinear_zpk`, then converted to transfer-function representation  $H(z) = B(z)/A(z)$  via `zpk2tf`. Coefficients are normalized so that  $a_0 = 1$  and  $|H(e^{j0})| = 1$ .

#### E. Selectivity and ROC Metrics

To quantify how steeply each filter transitions from passband to stopband, a selectivity factor

$$F_{ss} = \frac{N}{2\sqrt{2}\sqrt{W_p}\pi},$$

is used, where  $W_p = f_p/F_N$  is the normalized passband edge. For the same specifications, a lower  $F_{ss}$  corresponds to a narrower transition band and a more selective filter.

A region-of-convergence (ROC) indicator is also computed from prototype parameters and the order, giving a measure of how close the poles are to the unit circle.

### III. RESULTS ON THE SYNTHETIC TEST SIGNAL

#### A. Test Signal Definition

The synthetic test signal  $x[n]$  contains:

- a useful sinusoid at  $F_{\text{sig}} = 5$  kHz (unit amplitude, in the passband);
- a sinusoidal interference at  $F_{\text{int}} = 20$  kHz (amplitude 0.8, in the stopband);
- additive white Gaussian noise with standard deviation 0.5.

The signal has  $N = 10000$  samples at  $F_s = 50$  kHz.

#### B. Individual Filter Analysis

Figures 1 and 2 show the frequency responses and pole-zero locations. The Butterworth filter exhibits a smooth monotonic passband and a relatively gentle roll-off, while the Chebyshev-I filter has passband ripple but a much steeper attenuation beyond the passband edge.

#### C. Transition Band Comparison

Figure 3 compares the magnitude responses of the two filters on a normalized frequency axis. The smaller selectivity factor  $F_{ss}$  obtained for Chebyshev-I corresponds to the visibly sharper transition from passband to stopband.

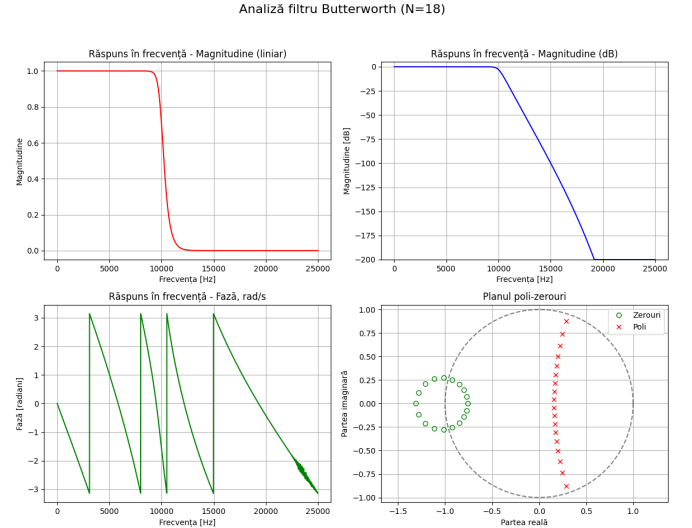


Fig. 1. Butterworth filter: magnitude (linear and dB), phase and pole-zero plot for the synthetic-signal design.

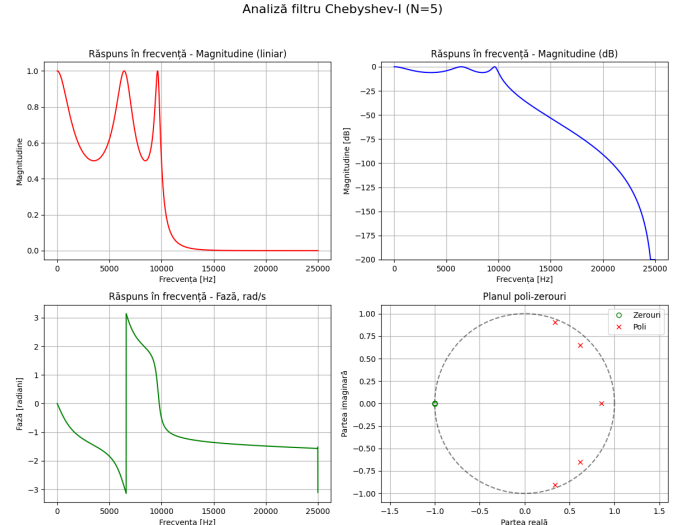


Fig. 2. Chebyshev-I filter: magnitude (linear and dB), phase and pole-zero plot for the synthetic-signal design.

#### D. Time- and Frequency-Domain Filtering Results

Figures 4 and 5 show the effect of each filter on the synthetic signal. Both preserve the 5 kHz component while strongly attenuating the 20 kHz interference and high-frequency noise, with the Chebyshev-I filter providing slightly stronger attenuation in the stopband.

### IV. ECG DENOISING EXPERIMENT

#### A. Dataset and Filter Specifications

For the second part of the project, the filters are applied to a real ECG signal. The signal comes from record 100 of a beginner-friendly version of the MIT-BIH arrhythmia database [2], provided as CSV files containing two ECG leads

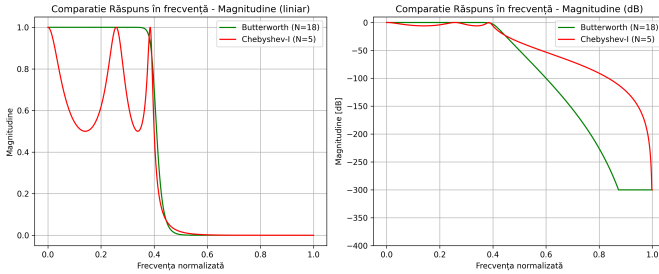


Fig. 3. Comparison of Butterworth and Chebyshev-I magnitude responses on normalized frequency, highlighting transition-band selectivity.

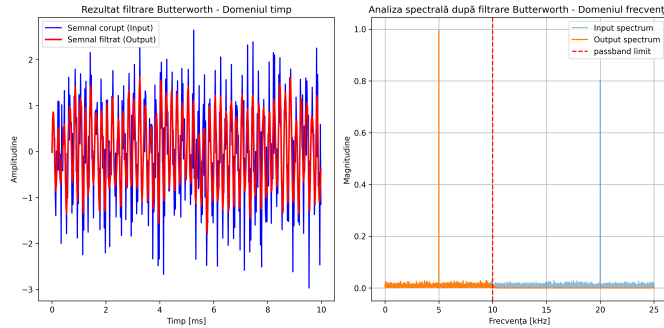


Fig. 4. Synthetic test signal: time-domain zoom and spectra before and after Butterworth filtering.

(MLII and V5), sampling frequency  $F_s = 360$  Hz and annotations. The script `test_data.py` reads `100_ekg.csv`, selects the MLII lead, and defines ECG-specific filter specifications:

- $F_s = 360$  Hz;
- $f_p = 40$  Hz, to preserve ECG morphology;
- $f_s = 60$  Hz, to strongly attenuate high-frequency noise and possible power-line components;
- $\delta_p = 0.5$ ,  $\delta_s = 34$ .

The same manual design functions are reused with these parameters, and zero-phase filtering is performed with `filtfilt`.

#### B. Time- and Frequency-Domain ECG Results

Figure 6 illustrates the effect of the Butterworth filter on the ECG signal; an analogous figure is generated for the Chebyshev-I filter. In both cases the high-frequency noise is significantly reduced while the main P–QRS–T complexes are preserved. Chebyshev-I tends to produce a slightly sharper attenuation of high-frequency components, consistent with the synthetic-signal results.

#### V. DISCUSSION AND CONCLUSIONS

The project demonstrates that manual design of Butterworth and Chebyshev-I IIR filters, followed by a careful digital realization via the bilinear transform, can be implemented compactly in Python and validated both on synthetic and real data. For the chosen specifications, the Chebyshev-I filter achieves a smaller selectivity factor and therefore a narrower

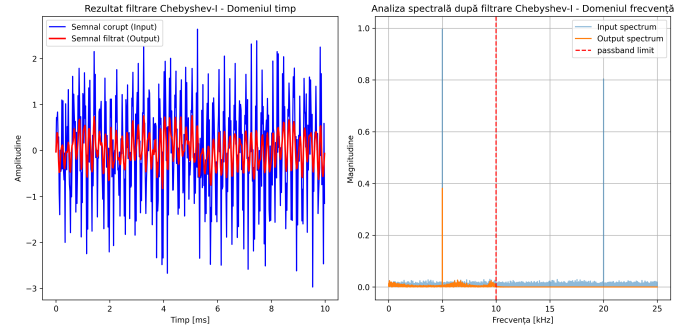


Fig. 5. Synthetic test signal: time-domain zoom and spectra before and after Chebyshev-I filtering.

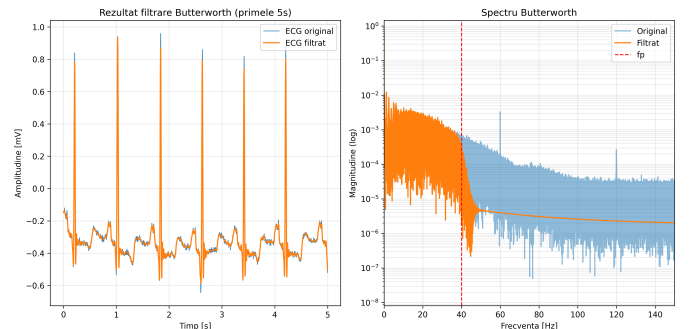


Fig. 6. ECG record 100, MLII lead: first 5 seconds and spectra before and after Butterworth filtering. (A similar plot is obtained for the Chebyshev-I filter.)

transition band than the Butterworth filter, at the cost of passband ripple. Both filters are stable, with poles strictly inside the unit circle.

On the synthetic test signal, both filters successfully suppress high-frequency sinusoidal interference and broadband noise while preserving the low-frequency sinusoid. On the ECG recording, they reduce high-frequency noise and make the heartbeat morphology more clearly visible without introducing noticeable distortions, which makes them suitable for ECG preprocessing tasks.

#### REFERENCES

- [1] S. K. Singh, A. Muhammad, I. Umaru, M. Usman, M. N. Abdulkareem, M. I. Abubakar, and M. Nur, "Computational Analysis of Butterworth and Chebyshev-I Filters Using Bilinear Transformation," *International Journal of Research – GRANTHAALAYAH*, vol. 10, pp. 37–56, 2022. Available: <https://doi.org/10.29121/granthaalayah.v10.i6.2022.4571>
- [2] G. B. Moody and R. G. Mark, "The Impact of the MIT-BIH Arrhythmia Database," *IEEE Engineering in Medicine and Biology Magazine*, vol. 20, no. 3, pp. 45–50, May–Jun. 2001. Available: <http://ecg.mit.edu/george/publications/mitdb-embs-2001.pdf>